crystals

MDPI

Article

Recyclable Carbon-Based Hybrid Adsorbents Functionalized with Alumina Nanoparticles for Water Remediation

Mohamed A. Habila [1,*], Zeid A. ALOthman [1], Hussam Musaad Hakami [1], Monerah R. ALOthman [2] and Mohamed Sheikh [1]

[1] Chemistry Department, College of Science, King Saud University, Riyadh 11451, Saudi Arabia
[2] Department of Botany and Microbiology, College of Science, King Saud University, Riyadh 11451, Saudi Arabia
* Correspondence: mhabila@ksu.edu.sa; Tel.: +966-1-4674-198; Fax: +966-1-4675-992

Abstract: Developing and improving adsorbent materials for wastewater treatment have become crucial for achieving recyclable water and keeping the environment safe. Carbon materials are modified with alumina (Al_2O_3) using various doping ratios and a solvothermal treatment. The process aims to combine the advantages of stable carbon and alumina materials with an efficient adsorbent for methylene blue removal. Fabricated materials including carbon and carbon/alumina derivatives were characterized with TEM, SEM, EDS, XRD, and FTIR, revealing successful surface modifications. The carbon materials exhibited pore diameters between 23 and 39 µm, while the modified ones showed pore diameters between 1.68 and 6.08 µm. The alumina nanoparticles were formed on a carbon surface with a particle size between 174 nm and 179 nm. Fabricated adsorbents were applied for the removal of methylene blue by adsorption at pH 4. The equilibrium and steady state adsorption stage was achieved after 2 h of reporting fast adsorption behavior. Low ratio carbon doping with alumina improved the adsorption capacity for methylene blue removal, while the excessive doping of carbon materials with alumina led to a reduction in adsorption efficiency. The application of pseudo-first-order and pseudo-second-order kinetic models indicated a fast adsorption mechanism, which agreed with the second-order model. The adsorption capacity for methylene blue was found to be 234 mg/g. Adsorption-isotherms including the Langmuir and Freundlich models were applied to investigate the adsorption mechanism. The results indicate that the Langmuir model fits with the adsorption data, which suggests a monolayer adsorption process.

Keywords: adsorption; recyclable carbon; alumina; methylene blue dye; water treatment; kinetic and isotherm modeling

check for updates

Citation: Habila, M.A.; ALOthman, Z.A.; Hakami, H.M.; ALOthman, M.R.; Sheikh, M. Recyclable Carbon-Based Hybrid Adsorbents Functionalized with Alumina Nanoparticles for Water Remediation. *Crystals* **2023**, *13*, 598. https://doi.org/10.3390/cryst13040598

Academic Editor: Chatchawal Wongchoosuk

Received: 15 February 2023
Revised: 22 March 2023
Accepted: 27 March 2023
Published: 1 April 2023

Copyright: © 2023 by the authors. Licensee MDPI, Basel, Switzerland. This article is an open access article distributed under the terms and conditions of the Creative Commons Attribution (CC BY) license (https://creativecommons.org/licenses/by/4.0/).

1. Introduction

Water pollution with dye leads to many negative environmental impacts and has been considered as an industrial hazard to urbanization in recent decades [1–5]. Methylene blue possesses a heterocyclic chemical structure of the molecular formula $C_{16}H_{18}N_3SCl$. Methylene blue has been extensively used for industrial coloring applications. Methylene blue dye applications extend to the coloring of paper, clothes, and leather. This leads to the contamination of industrial effluents and produces environmental, health, and surface water problems [6–8]. Methylene blue also has dangerous effects on ecosystems such as contaminating water resources and harming birds and animals. The most common side effects of consuming methylene blue are stomach upsets, diarrhea, vomiting, and bladder diseases. Symptoms also include turning urine or stools green-blue. Other dangerous side effects of methylene blue include dizziness, fainting, and fever. Individuals who are exposed to methylene blue should receive urgent medical attention to avoid complications or serious side effects [9,10].

Environmental regulation has led to the development of a number of wastewater treatment processes including photodegradation, bioremediation, adsorption, extraction,

and ion exchange [11–19]. Among these processes, many advantages for wastewater purification via the adsorptive removal of methylene blue have been reported including easy processing and low initial cost establishment [20]. Adsorption refers to the physical adhesion of chemicals onto the surface of a solid. Active carbon adsorption is regarded as the most commonly used technique for water treatment due to its ease and reliability [21–24]. Many adsorption applications have been investigated for their methylene blue removal from wastewater; for example, Kempson et al. investigated the adsorption of methylene blue using a silica-based adsorbent and reported on the effective interaction between the silica structure and S atom in the methylene blue dye [25]. Abdelfatah et al. reported on the green fabrication of iron with the application of Ricinus communis extracts for methylene blue removal from wastewater [26]. Gunture et al. used diesel soot to fabricate carbon for the adsorption of dyes [27]. Maruthapandi et al. applied carbon dots for the free radical-based fabrication of poly(4,4′-diaminodiphenylmethane) for methylene blue adsorption [28]. Hu et al. improved the adsorption of methylene blue by applying thermoresponsive polymers in hybrid network hydrogels [29]. Dhar et al. applied graphene oxide anchored Mg–Al-layered double hydroxides for the efficient adsorption of heavy metals and dyes, and reported that the mechanism of adsorption includes interactions of the S (dye) with H–O, S (dye) with O, and N (dye) with O–H, which were expected to stabilize methylene blue onto the surface of the graphene oxide anchored Mg–Al-layered double hydroxides [30]. Gautam and Hooda prepared magnetic graphene oxide/chitin nanocomposites for dye adsorption including methylene blue, recording an adsorption capacity of 332.61 mg/g [31].

The production of activated carbon is based on the application of natural or carbon rich materials such as coal or a waste-derived carbon skeleton, which has been exposed to chemical and physical activation processes [32–36]. A high temperature is a fundamental factor in the process of carbonization activation; at up to 600–1200 °C, it consumes a high level of energy. However, activation preparation is considered to be a cost-dependent process, especially in large amounts. Hence, there is an urgent need for other cheap materials to be used in water treatment instead of carbon [37–43]. The trend for fabrication of low-cost adsorbent materials is oriented toward recycling and processing either industrial or agricultural waste in order to produce carbon for adsorption and wastewater treatment applications [35,44,45].

Alumina-based materials have been reported as proper adsorbents for environmental pollutants [46–52]. Alumina exhibits high stability with a porous character, which enhances water treatment through adsorption applications using high selectivity and low-cost processing [53–56]. Although the fabrication of alumina anchored carbon adsorbents has previously been investigated, significant research in the relation to methods of fabrication as well as their utilization for various industrial and environmental applications is urgently required. Therefore, this study aimed to fabricate aluminum oxide nanoparticles with recyclable carbon from a waste source as a hybrid adsorbent using a solvothermal process. We sought to investigate and optimize the removal of methylene blue by adsorption onto fabricated adsorbents. Furthermore, we sought to apply the adsorption data with various kinetic and equilibrium isotherm models.

2. Materials and Methods

2.1. Fabrication of Alumina Nanoparticles Anchored with Recyclable Carbon-Based Hybrid Adsorbents

The chemicals and reagents used were of a high purity analytical grade. Aluminum nitrate, ammonium hydroxide, and methylene blue were purchased from Sigma Aldrich, USA. Recyclable carbon from a waste source (palm waste) (C-A-0) was prepared as previously described in our published works [57]. Then, 5 g of carbon was dispersed in a beaker containing 200 mL deionized water including 1.25 g aluminum nitrate to produce C-A-25, and the process was repeated with another aluminum nitrate ratio of 2.5 g to produce C-A-50. The mixtures were stirred for 1 h before ammonium hydroxide was added

to allow for the formation of aluminum hydroxide species on the carbon surfaces. The mixtures were then continuously stirred for an additional 3 h. The phases were separated by filtration. The carbon/aluminum species were heated in muffle furnaces in the near absence of oxygen at 600 °C to produce alumina nanoparticles anchored with recyclable carbon-based hybrid adsorbents. The structure and surface characteristics were examined by transmission electron microscopy (TEM) images, which were obtained using a JEOL JEM-2100F electron microscope (Japan), and the surface morphology was characterized by a scanning electron microscope (SEM) (JEOL GSM-7600F, Tokyo, Japan). Fourier transform infrared (FTIR) spectra were recorded using the Bruker Vertex-80 spectrometer to identify surface groups. The powder X-ray diffraction (XRD) patterns of PANalytical X'Pert PRO MPD (Almelo, The Netherlands) were recorded with Ni-filtered Cu Kα radiation (45 kV, 40 mA). In addition, a Micromeritics Gemini VII 2390 Surface Area and Porosity (Norcross, GA, USA) was used for the surface area measurements.

2.2. Application Studies for Adsorption of Methylene Blue onto Alumina Nanoparticles Anchored with Recyclable Carbon-Based Hybrid Adsorbents

A total of 0.05 g of the recyclable carbon C-A-0 and alumina nanoparticles anchored with recyclable carbon-based hybrid adsorbents (C-A-25 and C-A-50) were mixed with the methylene blue solution at a concentration of 50 mg/L. The pH of the mixture was adjusted to the desired pH using a phosphate buffer to adjust the pH of 2, 4, 5, 6, 7, and 8. The mixtures were separately shaken at 150 rpm for 2 h. Finally, the phases were separated by filtration and the methylene blue concentration was measured by UV–Visible spectroscopy. The adsorption capacity was calculated based on Equation (1):

$$qe = (C_0 - Cf) \cdot V/M, \quad (1)$$

where qe is the adsorption capacity (mg/g) of methylene blue onto the fabricated alumina nanoparticles anchored with recyclable carbon-based hybrid adsorbents.

C_0 refers to the initial concentration of methylene blue.

C_f is the final concentration of methylene blue after adsorption.

V is the volume of the adsorption medium.

M is the mass of the alumina nanoparticles anchored with recyclable carbon-based hybrid adsorbents (g).

To evaluate contact time effects, the same previous procedures were applied at time intervals of 15, 30, 45, 60, 120, 180, 240, 360, and 480 min. The adsorption conditions were adjusted to an adsorbent dose of 0.05 g, pH 4, and a methylene blue concentration of 50 mg/g. The adsorbent doses for C-A-0, C-A-25, and C-A-50 were similarly evaluated using 0.2, 0.3, 0.4, 0.5, 0.6, 0.7, and 0.8 g/L. The concentrations of methylene blue dye varied (25, 50, 80, 100, 150 and 200 mg/L) at pH 4, with a time of 120 min and an adsorbent dose of 0.05 and 150 rpm shaking conditions. Kinetic and isotherm models were used to assess the adsorbate/adsorbent equilibrium and predict the nature and rate of the adsorption process.

3. Results and Discussion

3.1. Characteristics of Alumina Nanoparticles Anchored with Recyclable Carbon-Based Hybrid Adsorbents

3.1.1. Microscopic Characterization of Alumina Nanoparticles Anchored with Recyclable Carbon-Based Hybrid Adsorbents

The surface structure of the prepared materials including the recyclable carbon (CA-0), alumina nanoparticles anchored with recyclable carbon-based hybrid adsorbent-25 (CA-25), and alumina nanoparticles anchored with recyclable carbon-based hybrid adsorbent-50 (CA-50) was examined by SEM, EDS, and TEM. The recyclable raw carbon materials exhibited a porous structure with the main surface elements C, O, and N (Figures 1 and 2). In addition, a perforated surface is clearly visible in Figure 2, with a pore diameter between 23 and 39 μm. The surface area of raw carbon materials was 568.1 m^2/g, which enabled an adsorption capacity for methylene blue removal of 201.8 mg/g (Table 1). The alumina

nanoparticles anchored with recyclable carbon-based hybrid adsorbent-25 (CA-25) showed the porous structure of carbon, with the addition of a surface structure from aluminum oxide, which was confirmed by the EDS analysis detecting C, O, N, and Al, which in turn were related to the presence of aluminum oxide on the surface of recyclable carbon materials (Figures 3 and 4). In addition, the formed particles of alumina on the carbon surfaces exhibited particle sizes between 174 and 179 nm (Figure 4), which was lower than that for the activated raw carbon materials (Figure 2). The surface area of CA-25 materials was 249.7 m^2/g, which enabled the adsorption capacity for the methylene blue removal of 234.4 mg/g, which was higher than that reported for activated raw carbon materials. Alumina nanoparticles anchored with recyclable carbon-based hybrid adsorbent-50 (CA-50) (Figures 5 and 6) were formed with a noticeable particulate on the surface of carbon, which was confirmed by the EDS analysis detecting C, O, N, and Al on the adsorbent surface. In addition, pores on the material surface were reported to have a diameter between 1.68 and 6.08 µm (Figure 6). The surface area of CA-50 materials was 247.0 m^2/g, which enabled the adsorption capacity for the methylene blue removal of 156.4 mg/g, which was the lowest compared to that reported for CA-25 and activated raw carbon materials. Al-Gaashani et al. reported a similar modification for the fabrication of carbon adorned with AlO_3 and Ag for the adsorption of molybdenum and arsenic, using the same morphological examination of the TEM and SEM images [58]. Such modifications of carbon materials make the surface rich with various electronegative atoms or compounds such as O, N, or Al; related oxide is expected to enhance interactions with pollutant molecules during adsorption and wastewater treatment, leading to the improved performance of adsorbent materials [55,59]. The results obtained in this study agree with the literature, which found that carbon pores are blocked at a higher doping ratio, leading to a lower porous structure but with higher efficiency [60,61].

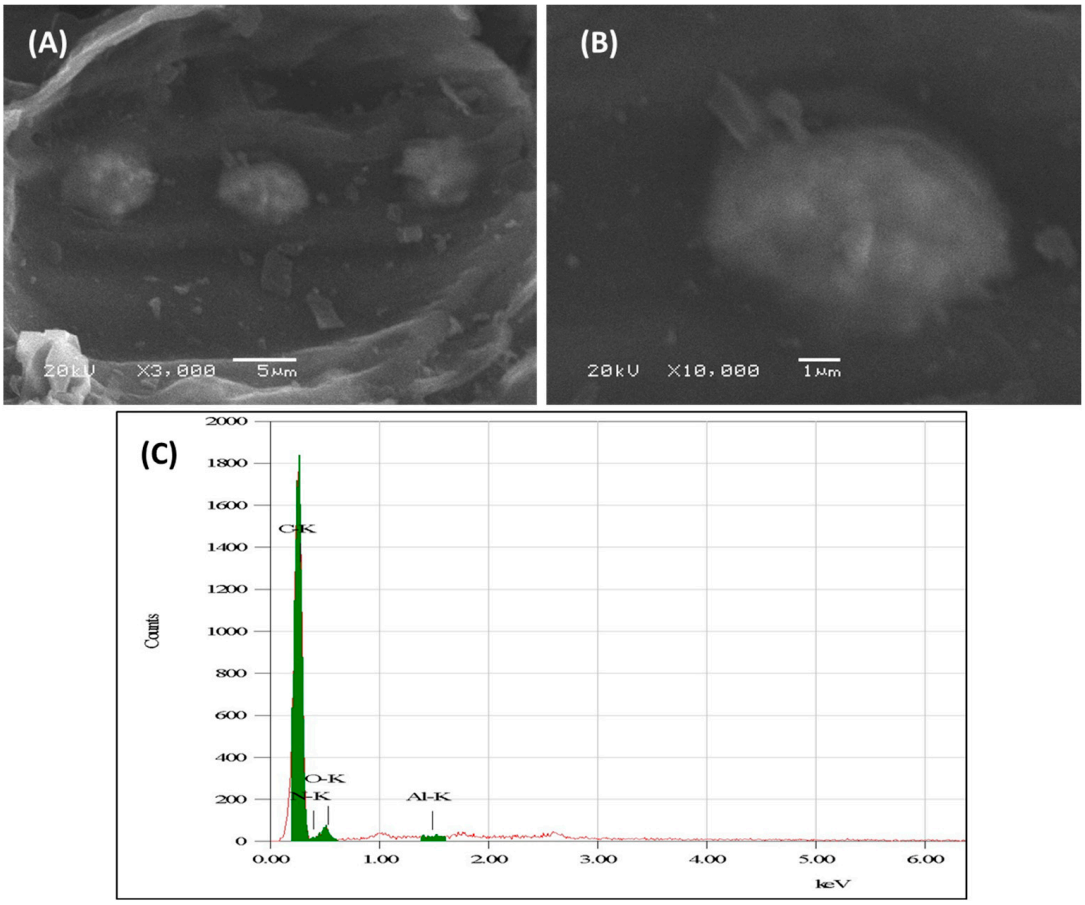


Figure 1. The SEM (**A**,**B**) and EDS (**C**) of the raw carbon materials.

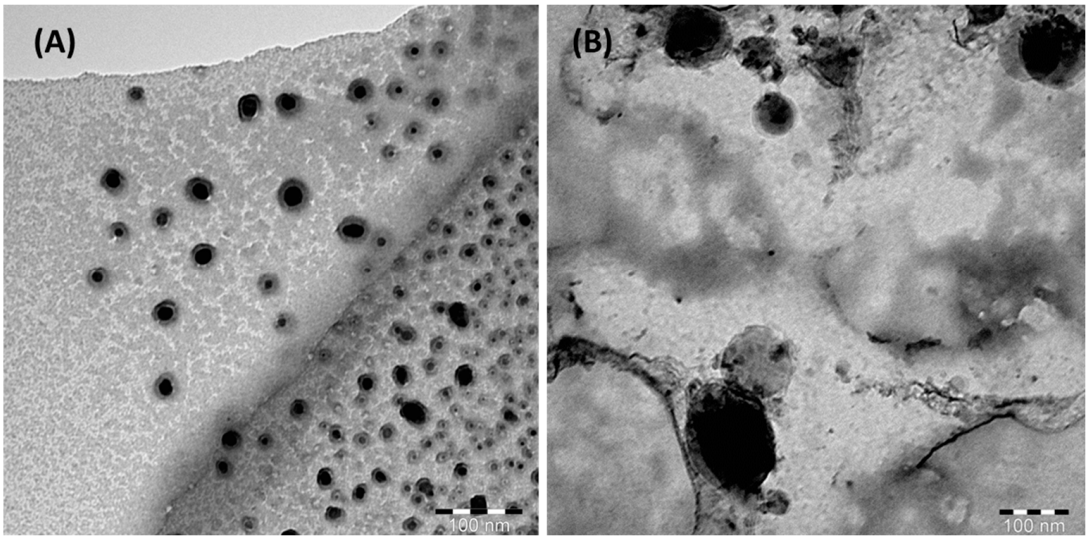


Figure 2. The TEM of the raw carbon materials (**A**,**B**) are for different places in the same sample.

Table 1. Surface areas and adsorption capacities for the alumina nanoparticles anchored with recyclable carbon-based hybrid adsorbent nanocomposites.

Adsorbent Materials	BET Surface Area (m^2/g)	Adsorption Capacity (mg/g)
C-A-0	568.1	201.8
C-A-25	249.7	234.4
C-A-50	247.0	156.4

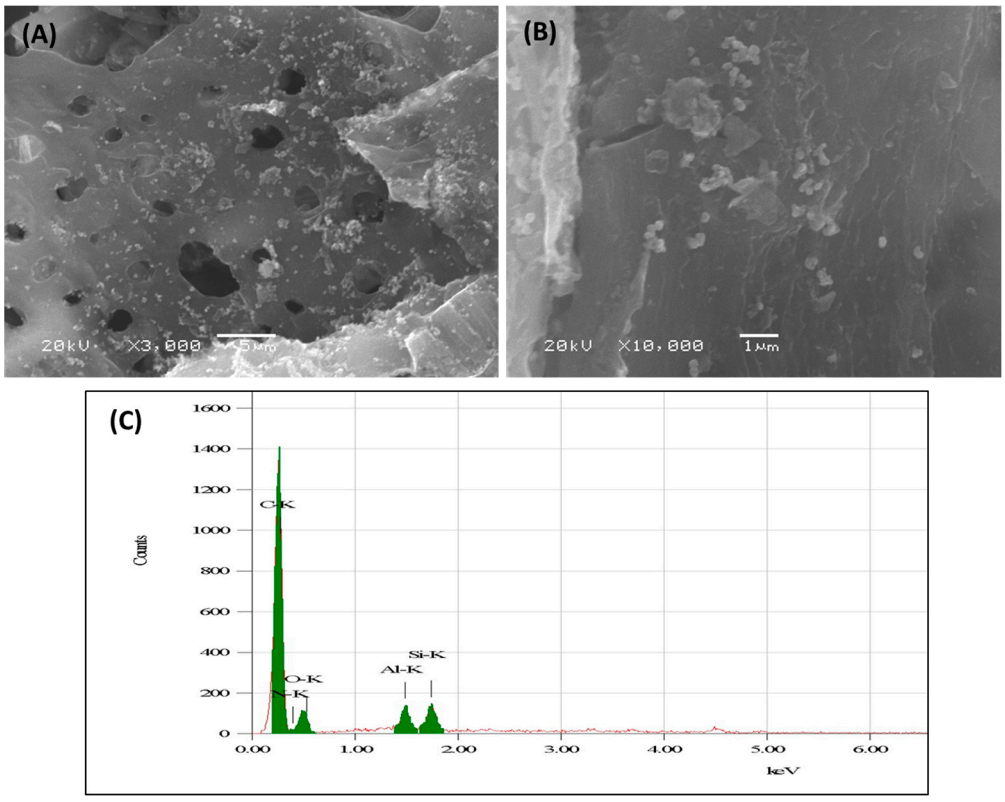


Figure 3. The SEM (**A**,**B**) and EDS (**C**) of alumina nanoparticles anchored with recyclable carbon-based hybrid adsorbent nanocomposites (C-A-25).

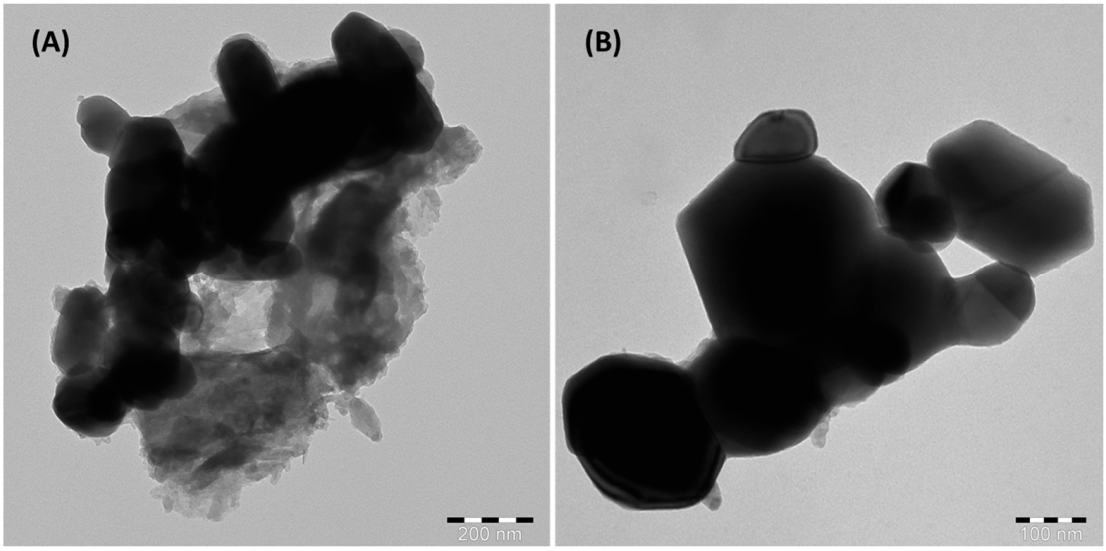


Figure 4. Transmission electron microscopy (TEM) of the alumina nanoparticles anchored with recyclable carbon-based hybrid adsorbent nanocomposites (C-A-25) at various scales of (**A**) 200 nm and (**B**) 100 nm.

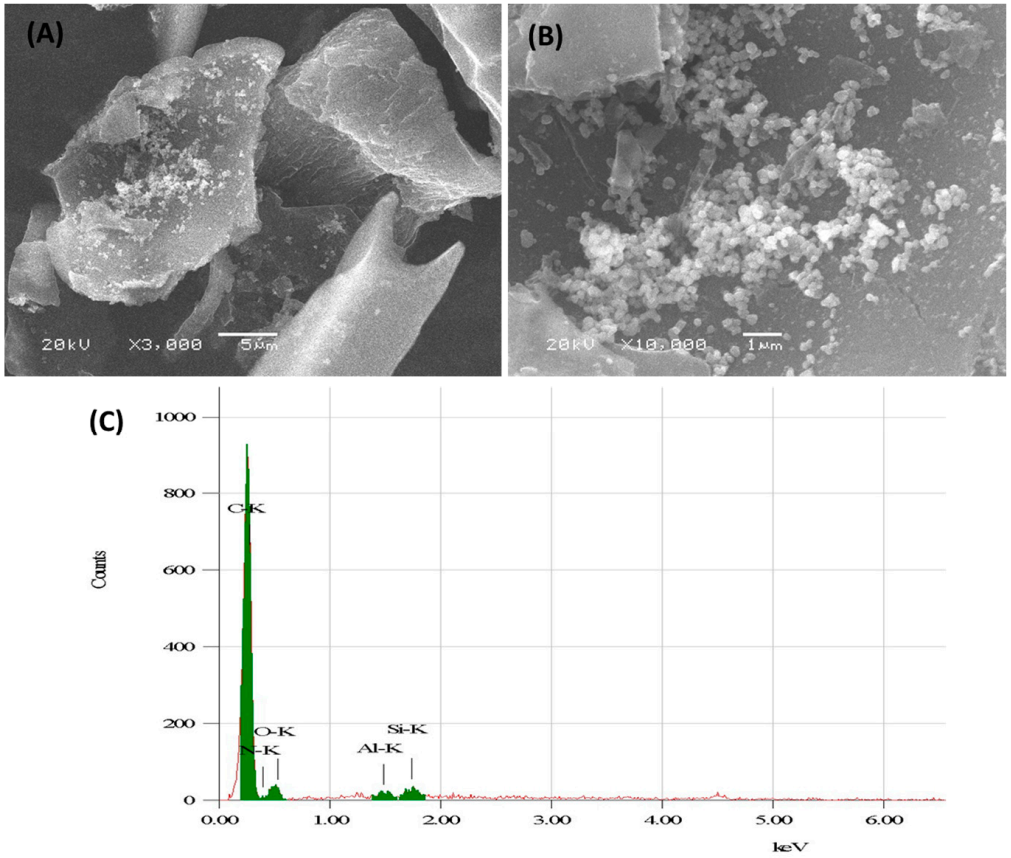


Figure 5. The SEM (**A**,**B**) and EDS (**C**) of the alumina nanoparticles anchored with recyclable carbon-based hybrid adsorbent nanocomposites (C-A-50).

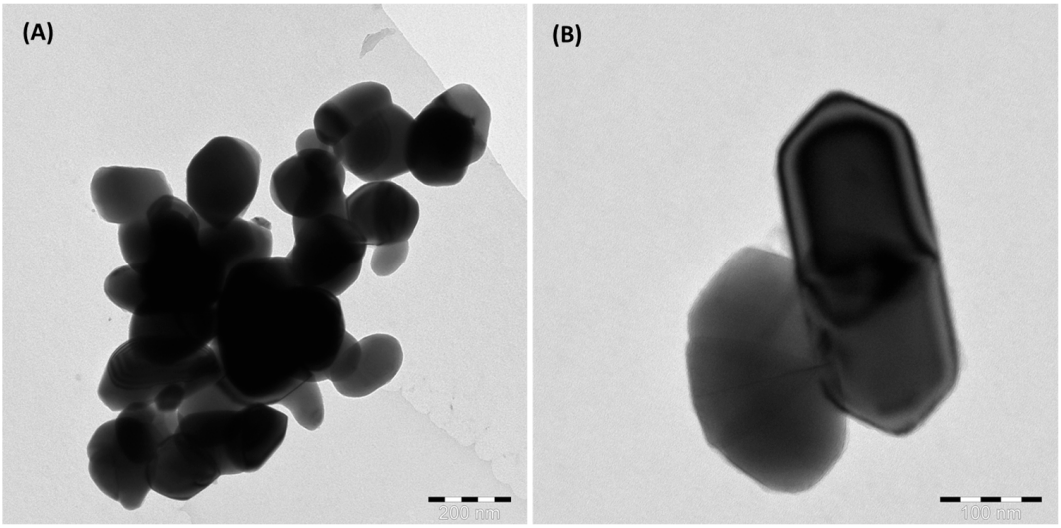


Figure 6. Transmission electron microscopy (TEM) of the alumina nanoparticles anchored with recyclable carbon-based hybrid adsorbent nanocomposites (C-A-50) at various scales of (**A**) 200 nm and (**B**) 100 nm.

3.1.2. Structural Characterization of Alumina Nanoparticles Anchored with Recyclable Carbon-Based Hybrid Adsorbents

The surface structure and functional groups of prepared materials including CA-0, CA-25, and CA-50 were examined by XRD (Figure 7). The detected XRD broad peak at two theta of 25 confirmed the amorphous structure of the samples due to the main carbon content of the materials. It has previously been reported that the carbon structures fabricated from waste sources exhibit an amorphous structure [62,63]. However, in cases of the modified samples of alumina nanoparticles anchored with recyclable carbon-based hybrid adsorbent-25 (CA-25) and alumina nanoparticles anchored with recyclable carbon-based hybrid adsorbent-50 (CA-50), some peaks were detected at about two theta of 27, 36, 38, 44, 54, 56, 61, and 68, corresponding to (012), (104), (110), (113), (024), (116), (018) and (214), respectively, due to the aluminum oxide modification [64,65]. In addition, low intensity peaks were reported for alumina modified samples due to the effect of the combination with a carbon structure.

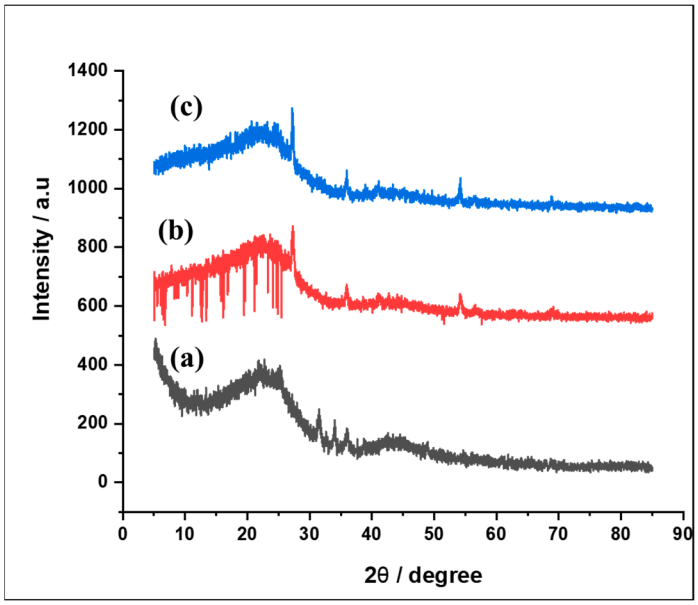


Figure 7. XRD analysis of (a) CA-0, (b) CA-25, and (c) CA-50.

The structure and functional groups on the surfaces of prepared materials—including the recyclable carbon (CA-0), alumina nanoparticles anchored with recyclable carbon-based hybrid adsorbent-25 (CA-25) and alumina nanoparticles anchored with recyclable carbon-based hybrid adsorbent-50 (CA-50)—were examined by FTIR (Figure 8). The recyclable carbon (CA-0) surfaces did not exhibit functional groups The spectrum showed peaks related to OH groups at about 3400 to 3600 cm^{-1} due to adsorbed OH groups in the cases of CA-25 and CA-50. In addition, the CH aliphatic appeared to be between 2800 and 2900 cm^{-1}. Furthermore, some peaks were detected at 518, 728 and 1060 cm^{-1} due to the Al-O of the aluminum oxide modification [65–67].

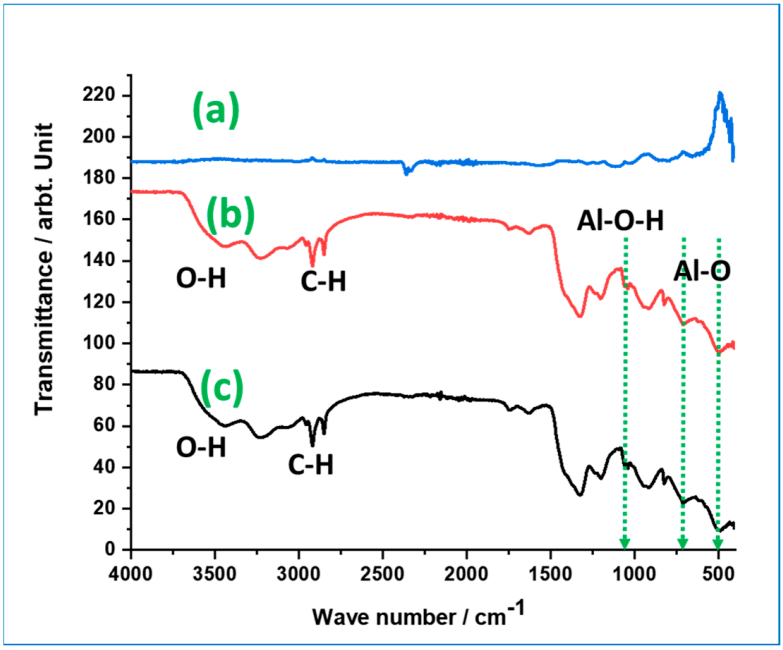


Figure 8. FTIR analysis of (a) recyclable carbon (CA-0), (b) CA-25, and (c) CA-50.

3.2. Adsorption Studies of Methylene Blue

3.2.1. Investigation of pH Effect

Methylene blue is considered to be a large, organic molecular weight pollutant, which is standard in nature and causes negative environmental impacts when released to water surfaces [19,21,32]. The adsorptive removal of methylene blue dye on the surface of an adsorbent is highly influenced by the surface charge and pH. We evaluated the pH effect on the tendency to adsorb methylene blue on the fabricated carbon and alumina nanoparticles anchored with recyclable carbon-based hybrid adsorbents in the range between 2 and 8. As shown in Figure 9, this was at an initial concentration of 53.65 mg/L. It is clear from this figure that for AC-0, AC-25, and AC-50, the maximum adsorption was at pH 4, while at a pH between 5 and 8, we noticed a decrease in the adsorption capacity. The pH of the methylene blue aqueous solution had an effect on the AC-0, AC-25, and AC-50 surface binding sites as well as on the ionization and/or protonation process of methylene blue dye molecules. In addition, AC-25 showed the best adsorption capacity, which may be attributed to the presence of aluminum oxide nanoparticles, enhancing the adsorption of methylene blue compared to the original carbon; by increasing the amount of aluminum oxide nanoparticles, carbon pores are blocked, leading to a decrease in adsorption efficiency [68]. The adsorption efficiency depends on the surface area as well as the surface functional groups. The reported surface area for AC-0, AC-25, and AC-50 was 568.1 m^2/g, 249.7 m^2/g, and 247.0 m^2/g, respectively (Table 1). The adsorption capacity in the case of AC-0 mainly depended on the surface area as the FTIR (Figure 8) showed no particular surface groups. while in the case of the modified adsorbents AC-25 and AC-50, the presence of Al-O and OH (Figure 8) may play the most important role for methylene blue adsorption.

The mechanism of the adsorption of methylene blue onto AC-0, AC-25, and AC-50 may include various electronegative atoms in adsorbents such as Al–O and OH and N and S atoms in methylene blue dye. These forces may include dipole–dipole interactions and/or Van der Waals forces.

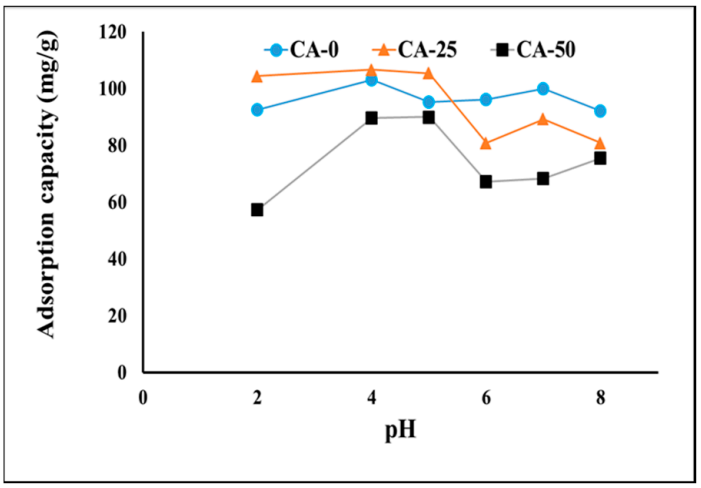


Figure 9. Influence of the initial pH of a methylene blue solution (50 mg/L) on the adsorption capacity of the prepared CA-0, CA-25, and CA-50 at a dose of 0.05 g, 25 °C and shaking rate of 150 rpm for 2 h.

3.2.2. Effect of Adsorbent Dose, Contact Time, and Kinetic Model Evaluation

The effect of the CA-0, CA-25, and CA-50 doses on the adsorption process was studied in the range between 0.2 g/L and 0.8 g/L, as shown in Figure 10A. The maximum adsorption capacities were between 150 and 234 mg/g for CA-0, CA-25, and CA-50, with the lowest reported for CA-50. The adsorption capacity was decreased by increasing the adsorbent dose because of the presence of unused adsorbent surfaces [57,69].

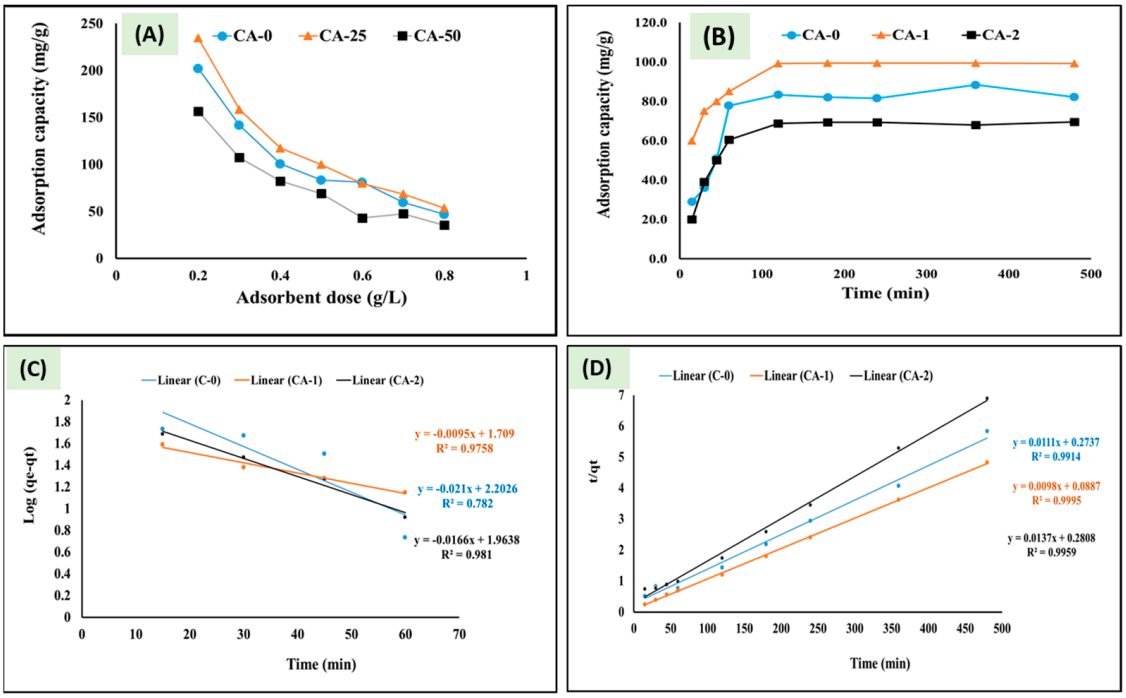


Figure 10. Optimization of the adsorption process of MB onto CA-0, CA-25, and CA-50: (**A**) adsorbent dose, (**B**) contact time, (**C**) pseudo-first-order kinetic model, and (**D**) pseudo-second-order kinetic model at a shaking rate of 150 rpm, 25 °C, and pH 4.

The amount of MB adsorbed onto CA-0, CA-25, and CA-50 was examined to evaluate the effect of time between 15 min and 480 min (Figure 10B). The adsorption capacity of methylene blue onto CA-0, CA-25, and CA-50 was increased by changing the time from 15 to 120 min, and after 120 min, there was no observed increase because the equilibrium state was reached. In addition, the adsorption capacities were 83.3 mg/g, 99.2 mg/g, and 68.8 mg/g for CA-0, CA-25, and CA-50 at the equilibrium state, using an adsorbent dose of 0.05 g, methylene blue concentration of 50 mg/L, 25 °C, and shaking rate of 150 rpm. Moreover, we investigated the methylene blue uptake by adsorption onto CA-0, CA-25, and CA-50 toward kinetic behavior using the pseudo-first-order and the pseudo-second-order in order to illustrate the process rate [70–73]. The integrated Equation (2) of the pseudo-first-order is:

$$\log(qe - qt) = \log qe - k_1 t/2.303 \quad (2)$$

where qe is the MB adsorption capacity at the time of equilibrium, while qt is related to the MB adsorption capacity at time t; k_1 is the kinetic rate constant in case of applying the pseudo-first-order reaction (min^{-1}) using the prepared materials of CA-0, CA-25, and CA-50.

Figure 10C shows the pseudo-first-order reaction as the relation of the log(qe − qt) as the y axes with t as the x axes, which enable the calculation of values k_1 and qe (Table 2).

Table 2. The kinetic parameters for the adsorption of methylene blue onto CA-0, CA-25, and CA-50.

		Pseudo-First-Order			Pseudo-Second-Order		
Adsorbent Materials	**qe,exp (mg/g)**	**K1 (min^{-1})**	**qe,cal (mg/g)**	**R^2**	**k2 (g/mg·min)**	**qe,cal (mg/g)**	**R^2**
C-0	83.3	0.048	159.4	0.782	4.5×0^{-4}	90.09	0.991
CA-1	99.2	0.021	51.1	0.975	1.08×10^{-3}	102.04	0.999
CA-2	68.8	0.038	92	0.981	6.68×10^{-4}	72.99	0.995

Furthermore, Equation (3) is the integrated pseudo-second-order kinetic equation:

$$t/qt = 1/kqe^2 + (1/qe) \times t \quad (3)$$

where t is the estimated contact time (min) and qe is in mg of methylene blue/g of the adsorbent including CA-0, CA-25, or CA-50. Moreover, qe^2 (mg/g) refers to the amount of methylene blue that was adsorbed at the time of equilibrium.

Figure 10D shows the graph plotting of t/qt with t, which enables the calculation of qe and k (Table 2). From the obtained results, the experimental q and calculated q values were found to be in good correlation, revealing that the pseudo-second-order kinetic model was well-fitted for describing the adsorption data of methylene blue uptake onto CA-0, CA-25, and CA-50. Based on these results, the mechanism of methylene blue adsorption onto recyclable carbon and alumina nanoparticles anchored with recyclable carbon-based hybrid adsorbents may include three steps: the migration of methylene blue in the solution, arrangement on the adsorbent surfaces, and migration in the entire pores of adsorbents. The three-phase adsorption process has been reported to be associated with second-order kinetic behavior during the adsorption of dyes and/or heavy metals. For example, El-Toni et al. reported the application of amino functionalized hollow core–mesoporous shell silica spheres for Pb(II), Cd(II), and Zn(II), which agreed with the second-order kinetics mechanism, with a suggestion of the three stage adsorption mechanism [74]. In addition, AlOthman et al. reported the removal of methylene blue using activated carbon from a mixed waste source, with suggested second-order kinetic model agreement [69].

3.2.3. Isotherm Studies

An analysis of the adsorption data in relation to concentration changes (25, 50, 80, 100, 150, and 200 mg/L) at a constant temperature, pH, shaking time, and adsorbent

dose is important to assess the nature of the arrangement of the methylene blue adsorbed molecules on the fabricated CA-0, CA-25, and CA-50 carbon derivatives.

- Langmuir isotherm [75]

The adsorption of methylene blue onto CA-0, CA-25, and CA-50 was studied using the Langmuir model, which is related to the monolayer formation of adsorbate around the applied CA-0, CA-25, and CA-50 adsorbents. The application of the isotherm model enables more information about the adsorption process and the behavior of the adsorbate during and after the process [76–80]. For example, the Langmuir model assumes that transmigration of the adsorbed ions is not assumed as happening on the plane surface. The application of Equation (4) for the Langmuir model for the uptake of methylene blue onto CA-0, CA-25, and CA-50 is presented in Figure 11A.

$$\frac{C_e}{q_e} = \left(\frac{1}{Q^0_{max}}\right)C_e + \frac{1}{Q^0_{max}K_L} \quad (4)$$

where Q^o_{max} is the adsorption capacity in its maximum value (mg/g) for the monolayer adsorption-capacity of methylene blue onto CA-0, CA-25, and CA-50; Ce (mg/L) is the methylene blue concentration at equilibrium; qe (mg/g) is the quantity of methylene blue at equilibrium; K_L (L/mg) is a constant associated with the affinity between an adsorbent and adsorbate.

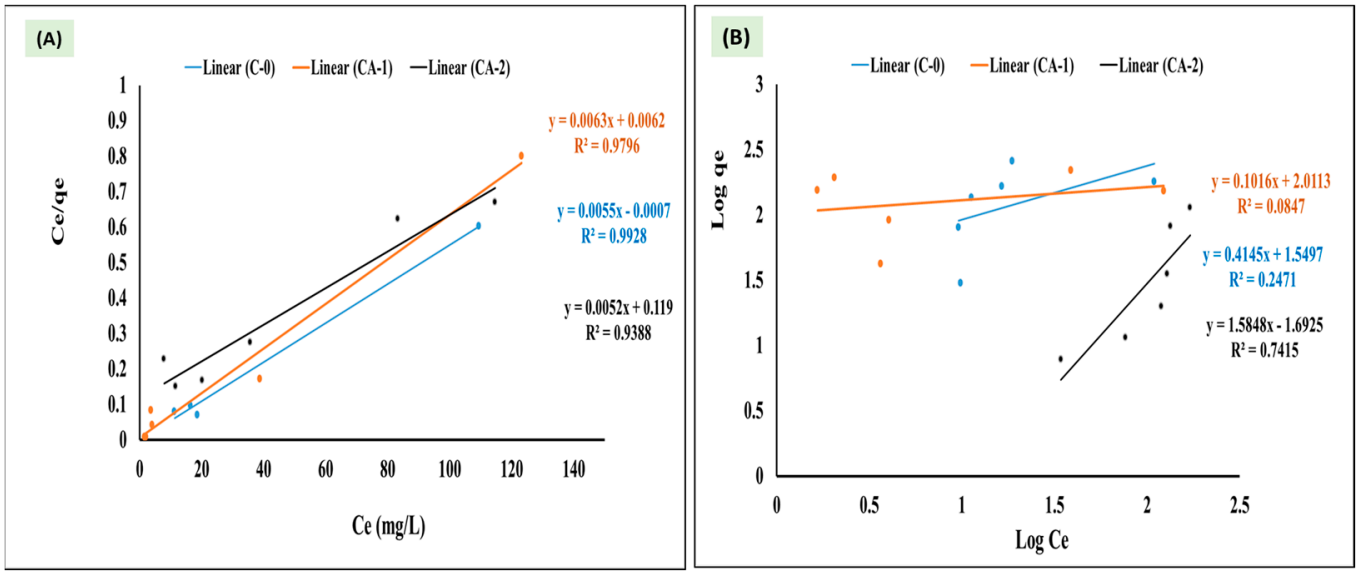


Figure 11. Equilibrium isotherms: (**A**) Langmuir isotherm and (**B**) Freundlich isotherm for the adsorption of initial methylene blue connotations of 25, 50, 80, 100, 150, and 200 mg/L onto CA-0, CA-25, and CA-50 at a dose of 0.5 g/L, 25 °C, and shaking rate of 150 rpm for 2 h.

The calculated correlation coefficient-R^2 for the adsorption of methylene blue onto CA-0, CA-25, and CA-50 (Figure 11A) (Table 3) had high values, indicating that the Langmuir model's assumption can be applied to describe the adsorption process.

Table 3. Isotherm parameters for the adsorption of methylene blue onto CA-0, CA-25, and CA-50.

	Langmuir Constants				Freundlich Constants		
	K_L	b	Q max.	R^2	K_F	n	R^2
C-0	60.86	7.8	181.8	0.9928	35.45	2.41	0.2471
CA-1	161.29	1.01	158.7	0.9796	102.63	9.84	0.0847
CA-2	4.37	0.04	192.3	0.9388	49.26	0.63	0.7415

- Freundlich isotherm [81]

  Equation (5) represents the Freundlich model:

$$\text{Logqe} = \text{logK} + 1/\text{n logCe} \quad (5)$$

where qe (mg/g) is the amount of methylene blue uptake onto CA-0, CA-25, and CA-50 at equilibrium, Ce (mg/L) is the methylene blue concentration at the time of equilibrium, KF $(mg/g)/(mg/L)^n$ is the Freundlich constant, and n is the Freundlich intensity parameter.

The K and n values were calculated by plotting log qe with log Ce, as presented in Figure 11B, and the results for applying the Freundlich model are set out in Table 3, which indicate that the model cannot be used for an applied adsorption process.

Disagreement of the adsorption data for methylene blue onto the fabricated recyclable carbon and alumina nanoparticles anchored with recyclable carbon-based hybrid adsorbents indicates that multi-layer adsorption is not the suggested mechanism. In addition, the chances for a monolayer adsorption mechanism are greater, according to the Langmuir assumptions [74].

4. Conclusions

Wastewater treatment by the adsorption of methylene blue dye was achieved by modified recyclable carbon materials. The solvothermal process was successfully applied to anchor aluminum oxide onto recyclable carbon materials. The hybrid aluminum oxide/carbon structures showed efficient adsorption performance for the removal of methylene blue with adsorption capacities between 150 and 234 mg/g. The adsorption process was found to follow the pseudo-second-order kinetic model and Langmuir isotherm. The adsorbent (CA-0, CA-25, and CA-50) doses were effectively influenced by the adsorption capacity for methylene blue removal, with the highest adsorption capacity being 0.2 g/L. The fabricated hybrid aluminum oxide/carbon structures will enhance future research applications related to the functionalization of waste-derived carbon materials with different metal oxide nanoparticles, which may serve catalysis, photocatalytic, and environmental applications. In addition, the prepared hybrid aluminum oxide/carbon structures can be utilized for broader adsorption applications for the separation of gases, polychlorinated biphenyls, pesticides, hydrocarbon, and/or pharmaceutical wastes.

Author Contributions: Conceptualization, M.A.H., H.M.H. and M.R.A.; Formal analysis, M.A.H., M.R.A. and M.S.; Investigation, M.A.H. and H.M.H.; Methodology, Z.A.A., H.M.H. and M.S.; Resources, Z.A.A. and M.R.A.; Supervision, Z.A.A.; Validation, M.A.H., Z.A.A. and M.S.; Writing—original draft, M.A.H. and M.S.; Writing—review & editing, M.A.H. and Z.A.A. All authors have read and agreed to the published version of the manuscript.

Funding: This research was funded by the National Plan for Science, Technology, and Innovation (MAARIFAH), King Abdulaziz City for Science and Technology, Kingdom of Saudi Arabia, grant number 3-17-01-001-0012.

Data Availability Statement: Samples of the compounds are available from the authors.

Acknowledgments: The authors acknowledge the National Plan for Science, Technology, and Innovation (MAARIFAH), King Abdulaziz City for Science and Technology, Kingdom of Saudi Arabia for its grant with award number 3-17-01-001-0012.

Conflicts of Interest: The authors declare no conflict of interest.

References

1. Bhatia, D.; Sharma, N.R.; Singh, J.; Kanwar, R.S. Biological methods for textile dye removal from wastewater: A review. *Crit. Rev. Environ. Sci. Technol.* **2017**, *47*, 1836–1876. [CrossRef]
2. Laing, I.G. The impact of effluent regulations on the dyeing industry. *Rev. Prog. Color. Relat. Top.* **2008**, *21*, 56–71. [CrossRef]
3. Forgacs, E.; Cserháti, T.; Oros, G. Removal of synthetic dyes from wastewaters: A review. *Environ. Int.* **2004**, *30*, 953–971. [CrossRef]
4. Ali, H. Biodegradation of synthetic dyes—A review. *Water Air Soil Pollut.* **2010**, *213*, 251–273. [CrossRef]

5. Mishra, S.; Cheng, L.; Maiti, A. The Utilization of agro-biomass/byproducts for effective bio-removal of dyes from dyeing wastewater: A comprehensive review. *J. Environ. Chem. Eng.* **2021**, *9*, 104901. [CrossRef]
6. Chandrasekhar, S.; Pramada, P.N. Rice husk ash as an adsorbent for methylene blue-effect of ashing temperature. *Adsorption* **2006**, *12*, 27–43. [CrossRef]
7. Feddal, I.; Ramdani, A.; Taleb, S.; Gaigneaux, E.M.; Batis, N.; Ghaffour, N. Adsorption capacity of methylene blue, an organic pollutant, by montmorillonite clay. *Desalin. Water Treat.* **2014**, *52*, 2654–2661. [CrossRef]
8. Hakami, A.A.H.; Wabaidur, S.M.; Khan, M.A.; AlOthman, Z.A.; Siddiqui, M.R. Extraction procedures and analytical methods for the determination of methylene blue, rhodamine B and crystal violet—An overview. *Curr. Anal. Chem.* **2020**, *17*, 708–728. [CrossRef]
9. Vutskits, L.; Briner, A.; Klauser, P.; Gascon, E.; Dayer, A.G.; Kiss, J.Z.; Muller, D.; Licker, M.J.; Morel, D.R. Adverse effects of methylene blue on the central nervous system. *Anesthesiology* **2008**, *108*, 684–692. [CrossRef]
10. Auerbach, S.S.; Bristol, D.W.; Peckham, J.C.; Travlos, G.S.; Hébert, C.D.; Chhabra, R.S. Toxicity and carcinogenicity studies of methylene blue trihydrate in F344N rats and B6C3F1 mice. *Food Chem. Toxicol.* **2010**, *48*, 169–177. [CrossRef]
11. Eslami, H.; Sedighi Khavidak, S.; Salehi, F.; Khosravi, R.; Fallahzadeh, R.A.; Peirovi, R.; Sadeghi, S. *Biodegradation of Methylene Blue from Aqueous Solution by Bacteria Isolated from Contaminated Soil*; Kurdistan University of Medical Sciences: Sanandaj, Iran, 2016; Volume 5.
12. Contreras, M.; Grande-Tovar, C.D.; Vallejo, W.; Chaves-López, C. Bio-removal of methylene blue from aqueous solution by galactomyces geotrichum KL20A. *Water* **2019**, *11*, 282. [CrossRef]
13. Mubarak, N.M.; Fo, Y.T.; Al-Salim, H.S.; Sahu, J.N.; Abdullah, E.C.; Nizamuddin, S.; Jayakumar, N.S.; Ganesan, P. Removal of methylene blue and orange-G from waste water using magnetic biochar. *Int. J. Nanosci.* **2015**, *14*, 1550009. [CrossRef]
14. Ong, S.A.; Toorisaka, E.; Hirata, M.; Hano, T. Biodegradation of redox dye methylene blue by up-flow anaerobic sludge blanket reactor. *J. Hazard. Mater.* **2005**, *124*, 88–94. [CrossRef]
15. El-Moselhy, M.M.; Kamal, S.M. Selective removal and preconcentration of methylene blue from polluted water using cation exchange polymeric material. *Groundw. Sustain. Dev.* **2018**, *6*, 6–13. [CrossRef]
16. Alkaykh, S.; Mbarek, A.; Ali-Shattle, E.E. Photocatalytic degradation of methylene blue dye in aqueous solution by MnTiO3 nanoparticles under sunlight irradiation. *Heliyon* **2020**, *6*, e03663. [CrossRef]
17. Habila, M.A.; Sheikh Moshab, M.; Mohamed El-Toni, A.; Al-Awadi, A.S.; ALOthman, Z.A. Facile Strategy for Fabricating an Organosilica-Modified Fe_3O_4 (OS/Fe_3O_4) Hetero-Nanocore and OS/Fe_3O_4@SiO_2 Core–Shell Structure for Wastewater Treatment with Promising Recyclable Efficiency. *ACS Omega* **2023**, *8*, 7626–7638. [CrossRef] [PubMed]
18. Taha, K.K.; al Zoman, M.; al Outeibi, M.; Alhussain, S.; Modwi, A.; Bagabas, A.A. Green and sonogreen synthesis of zinc oxide nanoparticles for the photocatalytic degradation of methylene blue in water. *Nanotechnol. Environ. Eng.* **2019**, *4*, 10. [CrossRef]
19. El-Ashtoukhy, E.S.Z.; Fouad, Y.O. Liquid-liquid extraction of methylene blue dye from aqueous solutions using sodium dodecylbenzenesulfonate as an extractant. *Alex. Eng. J.* **2015**, *54*, 77–81. [CrossRef]
20. Rafatullah, M.; Sulaiman, O.; Hashim, R.; Ahmad, A. Adsorption of methylene blue on low-cost adsorbents: A review. *J. Hazard. Mater.* **2010**, *177*, 70–80. [CrossRef]
21. Tong, D.S.; Wu, C.W.; Adebajo, M.O.; Jin, G.C.; Yu, W.H.; Ji, S.F.; Zhou, C.H. Adsorption of methylene blue from aqueous solution onto porous cellulose-derived carbon/montmorillonite nanocomposites. *Appl. Clay Sci.* **2018**, *161*, 256–264. [CrossRef]
22. Ghaedi, M.; Nasab, A.G.; Khodadoust, S.; Rajabi, M.; Azizian, S. Application of activated carbon as adsorbents for efficient removal of methylene blue: Kinetics and equilibrium study. *J. Ind. Eng. Chem.* **2014**, *20*, 2317–2324. [CrossRef]
23. Spagnoli, A.A.; Giannakoudakis, D.A.; Bashkova, S. Adsorption of methylene blue on cashew nut shell based carbons activated with zinc chloride: The role of surface and structural parameters. *J. Mol. Liq.* **2017**, *229*, 465–471. [CrossRef]
24. Fito, J.; Abrham, S.; Angassa, K. Adsorption of methylene blue from textile industrial wastewater onto activated carbon of parthenium hysterophorus. *Int. J. Environ. Res.* **2020**, *14*, 501–511. [CrossRef]
25. Kempson, I.M.; Barnes, T.J.; Prestidge, C.A. Use of TOF-SIMS to study adsorption and loading behavior of methylene blue and papain in a nano-porous silicon layer. *J. Am. Soc. Mass Spectrom.* **2010**, *21*, 254–260. [CrossRef] [PubMed]
26. Abdelfatah, A.M.; Fawzy, M.; Eltaweil, A.S.; El-Khouly, M.E. Green synthesis of nano-zero-valent iron using ricinus communis seeds extract: Characterization and application in the treatment of methylene blue-polluted water. *ACS Omega* **2021**, *6*, 25397–25411. [CrossRef] [PubMed]
27. Gunture; Kaushik, J.; Garg, A.K.; Saini, D.; Khare, P.; Sonkar, S.K. Pollutant diesel soot derived onion-like nanocarbons for the adsorption of organic dyes and environmental assessment of treated wastewater. *Ind. Eng. Chem. Res.* **2020**, *59*, 12065–12074. [CrossRef]
28. Maruthapandi, M.; Kumar, V.B.; Gedanken, A. Carbon dot initiated synthesis of poly(4,4′-diaminodiphenylmethane) and its methylene blue adsorption. *ACS Omega* **2018**, *3*, 7061–7068. [CrossRef] [PubMed]
29. Hu, N.; Chen, C.; Tan, J.; Wang, W.; Wang, C.; Fan, H.; Wang, J.; Müller-Buschbaum, P.; Zhong, Q. Enhanced adsorption of methylene blue triggered by the phase transition of thermoresponsive polymers in hybrid interpenetrating polymer network hydrogels. *ACS Appl. Polym. Mater.* **2020**, *2*, 3674–3684. [CrossRef]

30. Dhar, L.; Hossain, S.; Rahman, M.S.; Quraishi, S.B.; Saha, K.; Rahman, F.; Rahman, M.T. Adsorption mechanism of methylene blue by graphene oxide-shielded Mg-Al-layered double hydroxide from synthetic wastewater. *J. Phys. Chem. A* **2021**, *125*, 954–965. [CrossRef]
31. Harris, J.; Silk, R.; Smith, M.; Dong, Y.; Chen, W.T.; Waterhouse, G.I.N. Hierarchical TiO_2 Nanoflower photocatalysts with remarkable activity for aqueous methylene blue photo-oxidation. *ACS Omega* **2020**, *5*, 18919–18934. [CrossRef]
32. Vijayalaks, G.; Ramkumar, B.; Mohan, S.C. Isotherm and kinetic studies of methylene blue adsorption using activated carbon prepared from teak wood waste biomass. *J. Appl. Sci.* **2019**, *19*, 827–836. [CrossRef]
33. Heidarinejad, Z.; Rahmanian, O.; Fazlzadeh, M.; Heidari, M. Enhancement of methylene blue adsorption onto activated carbon prepared from date press cake by low frequency ultrasound. *J. Mol. Liq.* **2018**, *264*, 591–599. [CrossRef]
34. Xue, H.; Wang, X.; Xu, Q.; Dhaouadi, F.; Sellaoui, L.; Seliem, M.K.; ben Lamine, A.; Belmabrouk, H.; Bajahzar, A.; Bonilla-Petriciolet, A.; et al. Adsorption of methylene blue from aqueous solution on activated carbons and composite prepared from an agricultural waste biomass: A comparative study by experimental and advanced modeling analysis. *Chem. Eng. J.* **2022**, *430*, 132801. [CrossRef]
35. Habib Dakhil, I.; Ali, A.H. Adsorption of methylene blue dye from industrial wastewater using activated carbon prepared from agriculture wastes. *Desalin. Water Treat.* **2021**, *216*, 372–378. [CrossRef]
36. Pathania, D.; Sharma, S.; Singh, P. Removal of methylene blue by adsorption onto activated carbon developed from ficus carica bast. *Arab. J. Chem.* **2017**, *10*, S1445–S1451. [CrossRef]
37. Siddiqui, M.F.; Khan, S.A.; Hussain, D.; Tabrez, U.; Ahamad, I.; Fatma, T.; Khan, T.A. A sugarcane bagasse carbon-based composite material to decolor and reduce bacterial loads in waste water from textile industry. *Ind. Crops Prod.* **2022**, *176*, 114301. [CrossRef]
38. Primo, A.; Atienzar, P.; Sanchez, E.; Delgado, J.M.; García, H. From biomass wastes to large-area, high-quality, N-doped graphene: Catalyst-free carbonization of chitosan coatings on arbitrary substrates. *Chem. Commun.* **2012**, *48*, 9254–9256. [CrossRef]
39. Ilyas, M.; Ahmad, W.; Khan, H. Utilization of activated carbon derived from waste plastic for decontamination of polycyclic aromatic hydrocarbons laden wastewater. *Water Sci. Technol.* **2021**, *84*, 609–631. [CrossRef]
40. Karagoz, S.; Zengin, A.; Akalin, M.K.; Tekin, K.; Erdem, M.; Tay, T. Preparation and characterization of activated carbons from waste melamine coated chipboard by naoh activation. *Ekoloji* **2012**, *21*, 123–128. [CrossRef]
41. Zięzio, M.; Charmas, B.; Jedynak, K.; Hawryluk, M.; Kucio, K. Preparation and characterization of activated carbons obtained from the waste materials impregnated with phosphoric acid(V). *Appl. Nanosci.* **2020**, *10*, 4703–4716. [CrossRef]
42. Yu, J.; Zhang, D.; Zhu, S.; Chen, P.; Zhu, G.T.; Jiang, X.; Di, S. Eco-friendly and facile one-step synthesis of a three dimensional net-like magnetic mesoporous carbon derived from wastepaper as a renewable adsorbent. *RSC Adv.* **2019**, *9*, 12419–12427. [CrossRef] [PubMed]
43. Wu, H.; Chen, R.; Du, H.; Zhang, J.; Shi, L.; Qin, Y.; Yue, L.; Wang, J. Synthesis of activated carbon from peanut shell as dye adsorbents for wastewater treatment. *Adsorpt. Sci. Technol.* **2019**, *37*, 34–48. [CrossRef]
44. Zhang, Y.S.; Zhu, H.L.; Yao, D.; Williams, P.T.; Wu, C.; Xu, D.; Hu, Q.; Manos, G.; Yu, L.; Zhao, M.; et al. Thermo-Chemical Conversion of carbonaceous wastes for CNT and hydrogen production: A review. *Sustain. Energy Fuels* **2021**, *5*, 4173–4208. [CrossRef]
45. Li, L.Y.; Gong, X.D.; Abida, O. Waste-to-resources: Exploratory surface modification of sludge-based activated carbon by nitric acid for heavy metal adsorption. *Waste Manag.* **2019**, *87*, 375–386. [CrossRef]
46. Rastegar, A.; Farzadkia, M.; Jonoidi Jafari, A.; Esrafili, A. Preparation of carbon-alumina (C/Al_2O_3) aerogel nanocomposite for benzene adsorption from flow gas in fixed bed reactor. *MethodsX* **2019**, *6*, 2476–2483. [CrossRef]
47. Dao, T.H.; Vu, T.Q.M.; Nguyen, N.T.; Pham, T.T.; Nguyen, T.L.; Yusa, S.I.; Pham, T.D. Adsorption characteristics of synthesized polyelectrolytes onto alumina nanoparticles and their application in antibiotic removal. *Langmuir* **2020**, *36*, 13001–13011. [CrossRef]
48. Chen, A.S.C.; Snoeyink, V.L.; Fiessinger, F. Activated alumina adsorption of dissolved organic compounds before and after ozonation. *Environ. Sci. Technol.* **1987**, *21*, 83–90. [CrossRef]
49. Rahmani, A.; Mousavi, H.Z.; Fazli, M. Effect of nanostructure alumina on adsorption of heavy metals. *Desalination* **2010**, *253*, 94–100. [CrossRef]
50. Adesina, A.O.; Elvis, O.A.; Mohallem, N.D.S.; Olusegun, S.J. Adsorption of Methylene Blue and Congo Red from Aqueous Solution Using Synthesized Alumina–Zirconia Composite. *Environ. Technol.* **2019**, *42*, 1061–1070. [CrossRef]
51. Nédez, C.; Ray, J.L. Efficient removal of polymerization inhibitors by adsorption on the surface of an optimized alumina. *Langmuir* **1999**, *15*, 5932–5936. [CrossRef]
52. Mckinney, C.M.; Hopkins, R.L. Alumina-adsorption analysis of petroleum aromatics in 420° to 600° F. Range. *Anal. Chem.* **1954**, *26*, 1460–1465. [CrossRef]
53. Yobanny Reyes-López, S.; Arely Aguirre-Terrazas, K.; Torres-Pérez, J.; Nahúm, M.-C.; de Jesús Ruíz-Baltazar, Á. Review of alumina in adsorption processes for emerging pollutants. *Int. J. Res. GRANTHAALAYAH* **2021**, *9*, 435–453. [CrossRef]
54. Dambies, L. Existing and prospective sorption technologies for the removal of arsenic in water. *Sep. Sci. Technol.* **2005**, *39*, 603–627. [CrossRef]

55. Mohammadifar, E.; Shemirani, F.; Majidi, B.; Ezoddin, M. Application of Modified Nano-γ-Alumina as an Efficient Adsorbent for Removing Malachite Green (MG) from Aqueous Solution. *New Pub Balaban* **2014**, *54*, 758–768. [CrossRef]
56. Weidner, E.; Ciesielczyk, F. Removal of hazardous oxyanions from the environment using metal-oxide-based materials. *Materials* **2019**, *12*, 927. [CrossRef] [PubMed]
57. Habila, M.A.; Alothman, Z.A.; Ali, R.; Ghafar, A.A.; Hassouna, M.S.E.-D. Removal of tartrazine dye onto mixed-waste activated carbon: Kinetic and thermodynamic studies. *Clean* **2014**, *42*, 1824–1831. [CrossRef]
58. Al-Gaashani, R.; Almasri, D.; Shomar, B.; Kochkodan, V. Preparation and properties of novel activated carbon doped with aluminum oxide and silver for water treatment. *J. Alloys Compd.* **2021**, *858*, 158372. [CrossRef]
59. Ihsanullah; Asmaly, H.A.; Saleh, T.A.; Laoui, T.; Gupta, V.K.; Atieh, M.A. Enhanced adsorption of phenols from liquids by aluminum oxide/carbon nanotubes: Comprehensive study from synthesis to surface properties. *J. Mol. Liq.* **2015**, *206*, 176–182. [CrossRef]
60. Fatima, S.S.; Borhan, A.; Ayoub, M.; Ghani, N.A. CO_2 adsorption performance on surface-functionalized activated carbon impregnated with pyrrolidinium-based ionic liquid. *Processes* **2022**, *10*, 2372. [CrossRef]
61. Yusuf, N.Y.M.; Masdar, M.S.; Isahak, W.N.R.W.; Nordin, D.; Husaini, T.; Majlan, E.H.; Wu, S.Y.; Rejab, S.A.M.; Lye, C.C. Impregnated carbon–ionic liquid as innovative adsorbent for H_2/CO_2 separation from biohydrogen. *Int. J. Hydrogen Energy* **2019**, *44*, 3414–3424. [CrossRef]
62. Habila, M.A.; ALOthman, Z.A.; ALOthman, M.R.; Hassouna, M.S.E.D. Benzothiophene adsorptive desulfurization onto Trihexyl(tetradecyl)phosphonium dicyanamide ionic-liquid-modified renewable carbon: Kinetic, equilibrium and UV spectroscopy investigations. *Molecules* **2023**, *28*, 298. [CrossRef] [PubMed]
63. Habila, M.; AlOthman, Z.; Ghfar, A.; Al-Zaben, M.; Alothman, A.; Abdeltawab, A.; El-Marghany, A.; Sheikh, M. Phosphonium-based ionic liquid modified activated carbon from mixed recyclable waste for mercury(II) uptake. *Molecules* **2019**, *24*, 570. [CrossRef] [PubMed]
64. Borrell, A.; Rocha, V.G.; Torrecillas, R.; Fernández, A. Surface coating on carbon nanofibers with alumina precursor by different synthesis routes. *Compos. Sci. Technol.* **2011**, *71*, 18–22. [CrossRef]
65. Romero Toledo, R.; Ruiz Santoyo, V.; Moncada Sánchez, C.D.; Martínes Rosales, M. Effect of aluminum precursor on physicochemical properties of Al_2O_3 by hydrolysis/precipitation method. *Nova Sci.* **2018**, *10*, 83–99. [CrossRef]
66. Prashanth, P.A.; Raveendra, R.S.; Hari Krishna, R.; Ananda, S.; Bhagya, N.P.; Nagabhushana, B.M.; Lingaraju, K.; Raja Naika, H. Synthesis, characterizations, antibacterial and photoluminescence studies of solution combustion-derived α-Al 2 O 3 nanoparticles. *J. Asian Ceram. Soc.* **2015**, *3*, 345–351. [CrossRef]
67. Liu, C.; Shih, K.; Gao, Y.; Li, F.; Wei, L. Dechlorinating transformation of propachlor through nucleophilic substitution by dithionite on the surface of alumina. *J. Soils Sediments* **2012**, *12*, 724–733. [CrossRef]
68. Al-Marghany, A.; Badjah Hadj Ahmed, A.Y.; Alothman, Z.A.; Sheikh, M.; Ghfar, A.A.; Habila, M. Fabrication of schiff's base-functionalized porous carbon materials for the effective removal of toxic metals from wastewater. *Arab. J. Geosci.* **2021**, *14*, 336. [CrossRef]
69. AlOthman, Z.A.; Habila, M.A.; Ali, R.; Abdel Ghafar, A.; El-din Hassouna, M.S. Valorization of two waste streams into activated carbon and studying its adsorption kinetics, equilibrium isotherms and thermodynamics for methylene blue removal. *Arab. J. Chem.* **2014**, *7*, 1148–1158. [CrossRef]
70. Wu, F.C.; Tseng, R.L.; Juang, R.S. Kinetic modeling of liquid-phase adsorption of reactive dyes and metal ions on chitosan. *Water Res.* **2001**, *35*, 613–618. [CrossRef]
71. Bhatti, H.N.; Safa, Y.; Yakout, S.M.; Shair, O.H.; Iqbal, M.; Nazir, A. Efficient removal of dyes using carboxymethyl cellulose/alginate/polyvinyl alcohol/rice husk composite: Adsorption/desorption, kinetics and recycling studies. *Int. J. Biol. Macromol.* **2020**, *150*, 861–870. [CrossRef]
72. Elmoubarki, R.; Mahjoubi, F.Z.; Tounsadi, H.; Moustadraf, J.; Abdennouri, M.; Zouhri, A.; el Albani, A.; Barka, N. Adsorption of textile dyes on raw and decanted moroccan clays: Kinetics, equilibrium and thermodynamics. *Water Resour. Ind.* **2015**, *9*, 16–29. [CrossRef]
73. Hosseini, F.; Sadighian, S.; Hosseini-Monfared, H.; Mahmoodi, N.M. Dye removal and kinetics of adsorption by magnetic chitosan nanoparticles. *Desalin. Water Treat.* **2016**, *57*, 24378–24386. [CrossRef]
74. Mohamed El-Toni, A.; Habila, M.A.; Abbas Ibrahim, M.; Puzon Labis, J.; ALOthman, Z.A. Simple and facile synthesis of amino functionalized hollow Core-mesoporous shell silica spheres using anionic surfactant for Pb(II), Cd(II), and Zn(II) adsorption and recovery. *Chem. Eng. J.* **2014**, *251*, 441–451. [CrossRef]
75. Langmuir, I. The constitution and fundamental properties of solids and liquids. Part I. Solids. *J. Am. Chem. Soc.* **1916**, *38*, 2221–2295. [CrossRef]
76. Ayawei, N.; Ebelegi, A.N.; Wankasi, D. Modelling and interpretation of adsorption isotherms. *J. Chem.* **2017**, *2017*, 3039817. [CrossRef]
77. Saleh, T.A.; Al-Absi, A.A. Kinetics, isotherms and thermodynamic evaluation of amine functionalized magnetic carbon for methyl red removal from aqueous solutions. *J. Mol. Liq.* **2017**, *248*, 577–585. [CrossRef]
78. Myneni, V.R.; Kanidarapu, N.R.; Vangalapati, M. Methylene blue adsorption by magnesium oxide nanoparticles immobilized with chitosan (CS-MgONP): Response surface methodology, isotherm, kinetics and thermodynamic studies. *Iran. J. Chem. Chem. Eng.* **2020**, *39*, 29–42.

79. Ghate, E.; Ganjidoust, H.; Ayati, B. The thermodynamics, kinetics, and isotherms of sulfamethoxazole adsorption using magnetic activated carbon nanocomposite and its reusability potential. *Nanotechnol. Environ. Eng.* **2021**, *6*, 32. [CrossRef]
80. Wang, S.; Zhai, Y.Y.; Gao, Q.; Luo, W.J.; Xia, H.; Zhou, C.G. Highly efficient removal of acid red 18 from aqueous solution by magnetically retrievable chitosan/carbon nanotube: Batch study, isotherms, kinetics, and thermodynamics. *J. Chem. Eng. Data* **2014**, *59*, 39–51. [CrossRef]
81. Freundlich, H.M.F. Over the adsorption in solution. *J. Phys. Chem. A* **1906**, *57*, 385–470.

Disclaimer/Publisher's Note: The statements, opinions and data contained in all publications are solely those of the individual author(s) and contributor(s) and not of MDPI and/or the editor(s). MDPI and/or the editor(s) disclaim responsibility for any injury to people or property resulting from any ideas, methods, instructions or products referred to in the content.